Journal of Cerebral Blood Flow & Metabolism (2013) 33, 1582–1594

www.jcbfm.com

ORIGINAL ARTICLE

Regenerative glutamate release by presynaptic NMDA receptors contributes to spreading depression

Ning Zhou[1,2,3], Ravi L Rungta[1], Aqsa Malik[1], Huili Han[1], Dong Chuan Wu[1,2,3] and Brian A MacVicar[1]

Spreading depression (SD) is a slowly propagating neuronal depolarization that underlies certain neurologic conditions. The wave-like pattern of its propagation suggests that SD arises from an unusual form of neuronal communication. We used enzyme-based glutamate electrodes to show that during SD induced by transiently raising extracellular K^+ concentrations ($[K^+]_o$) in rat brain slices, there was a rapid increase in the extracellular glutamate concentration that required vesicular exocytosis but unlike fast synaptic transmission, still occurred when voltage-gated sodium and calcium channels (VGSC and VGCC) were blocked. Instead, presynaptic *N*-methyl-D-aspartate (NMDA) receptors (NMDARs) were activated during SD and could generate substantial glutamate release to support regenerative glutamate release and propagating waves when VGSCs and VGCCs were blocked. In calcium-free solutions, high $[K^+]_o$ still triggered SD-like waves and glutamate efflux. Under such a condition, glutamate release was blocked by mitochondrial Na^+/Ca^{2+} exchanger inhibitors that likely blocked calcium release from mitochondria secondary to NMDA-induced Na^+ influx. Therefore presynaptic NMDA receptor activation is sufficient for triggering vesicular glutamate release during SD via both calcium entry and release from mitochondria by mitochondrial Na^+/Ca^{2+} exchanger. Our observations suggest that presynaptic NMDARs contribute to a cycle of glutamate-induced glutamate release that mediate high $[K^+]_o$-triggered SD.

Journal of Cerebral Blood Flow & Metabolism (2013) **33,** 1582–1594; doi:10.1038/jcbfm.2013.113; published online 3 July 2013

Keywords: glutamate release; presynaptic NMDA receptors; spreading depression

INTRODUCTION

Spreading depression (SD, also termed spreading depolarization) is a slowly propagating wave of neuronal depolarization that contributes to damage expansion after several neurologic conditions like malignant hemispheric stroke, subarachnoid hemorrhage, intracranial hemorrhage, and brain trauma.[1,2] Although SD is mostly observed in damaged brains clinically, it can also be evoked in healthy tissues by various stimuli. A profound depolarization occurs at the SD wave front, which inactivates voltage-gated ion channels and causes SD of brain electrical activity.[3] *N*-methyl-D-aspartate receptors (NMDARs) are generally believed critical for SD propagation, as SD can be suppressed by its antagonists and evoked by its agonists.[2] The role of NMDARs in SD is commonly explained by the 'glutamate hypothesis', which suggests that SD is triggered by intensive release of glutamate that activates postsynaptic NMDARs and thereby evokes further neuronal firing and glutamate release, forming a positive feedback cycle. However, important questions remain unanswered. For instance, action potentials and evoked synaptic responses are not thought to be responsible for SD, because most voltage-gated sodium channels (VGSC) quickly inactivate before the SD wave reaches the maximal amplitude of depolarization.[4] Although cortical SD induced by focal potassium injection is prevented by blocking voltage-gated calcium channels (VGCC), especially P/Q-type channels,[5,6] some types of propagating SD can be elicited even after pharmacological blockade of VGCC-mediated calcium influx or in solution with 0 external Ca^{2+} concentration (0 $[Ca^{2+}]_o$).[7,8] The independence of VGSC and VGCC activation also makes it difficult to explain how activation of postsynaptic NMDARs in dendrites causes glutamate release at distant presynaptic sites to maintain SD.

Recent compelling anatomic evidence has demonstrated that NMDARs are expressed at presynaptic terminals in various regions including the neocortex and hippocampus.[9,10] Electrophysiological recordings have shown that presynaptic NMDARs facilitate both spontaneous and evoked neurotransmitter release.[9,11] Focal glutamate uncaging directly induced presynaptic NMDAR currents in the hippocampal pyramidal cell boutons.[10] Based on these findings, we hypothesized that activation of presynaptic NMDARs could directly trigger more glutamate release and further activate more presynaptic NMDARs thereby contributing to glutamate release during SD. Under some conditions, glutamate may diffuse to activate NMDARs on adjacent presynaptic terminals, evoking further release at these sites and thereby generating a propagating wave of regenerative glutamate release. Such a mechanism could mediate the propagation of SD under certain circumstances like high $[K^+]_o$.

In this study, we used enzyme-based glutamate electrodes in combination with electrophysiological recordings and intrinsic optical signals (IOS) to examine the contribution of different mechanisms to the glutamate release during an SD-like propagating wave triggered by high $[K^+]_o$ in brain slices. We report that

[1]Brain Research Centre, Department of Psychiatry, University of British Columbia, Vancouver, British Columbia, Canada; [2]Translational Medicine Research Center, China Medical University Hospital, Taichung, Taiwan and [3]China Medical University, Taichung, Taiwan. Correspondence: Dr BA MacVicar, Brain Research Centre, Department of Psychiatry, University of British Columbia, 2211 Wesbrook Mall Vancouver, Vancouver, BC, Canada V6T 2B5.
E-mail: bmacvicar@brain.ubc.ca
This work was supported by grants to BAM from the Canadian Institutes of Health Research (MOP-8545, MOP-11512 and TCE-117869 in the framework of the ERA-NET NEURON), by Taiwan National Science Council (NSC 100-2632-B-039-001-MY3 and NSC101-2314-B-039-001), by CMUH DMR-101-121, and in part by Taiwan Department of Health Clinical Trial and Research Center of Excellence (DOH102-TD-B-111-004).
Received 13 March 2013; revised 10 June 2013; accepted 13 June 2013; published online 3 July 2013

when SD was induced by high $[K^+]_o$ solutions, SD propagation was mediated by vesicular glutamate release triggered by presynaptic NMDARs independent of VGSCs or VGCCs. Our observations support the notion that a presynaptic NMDAR-dependent mechanism can contribute to and under some circumstances underlie a vicious cycle of glutamate-induced glutamate release to promote the propagation of SD induced by high $[K^+]_o$ treatments.

MATERIALS AND METHODS

Slice Preparation and Induction of Spreading Depression

Experimental protocols were approved by the University of British Columbia Animal Care Committee and conformed to the Canadian Council on Animal Care and Use guidelines, and were evaluated and approved by the Institutional Animal Care and Use Committee of China Medical University according to Care of the Animals and Surgical Procedures of China Medical University Protocols. Rats were anesthetized with halothane, decapitated, and the brains removed into ice-cold slicing solution. Transverse hemi-sections, 400 μm thick, from the hippocampus or cortical hemi-sections from the neocortex/striatum were prepared from 19- to 23-day old Sprague–Dawley rats of either sex. Then the slices were transferred to a storage chamber and incubated with fresh artificial cerebrospinal fluid (ACSF). Spreading depression was induced by perfusing high $[K^+]_o$ solution (containing 40 mmol/L K^+) at 3 mL/minute.

Recording Spreading Depression Propagation

Intrinsic optical signals data were collected from the transmitted light of brain slices by a CCD camera (DAGE-MTI) connected to a DT3155 frame grabber (Data Translation) controlled by Imaging Workbench 5.0 software (INDEC, Santa Clara, CA, USA). The illumination source was a standard Zeiss tungsten bulb whose output was directed through a 750DF20 filter. In all the experiments, the IOS' were recorded simultaneously with real time glutamate measurements to indicate the onset and propagation of SD (Figure 1).[8]

Glutamate Measurement

Real time glutamate concentration changes were detected by enzyme-based microelectrode arrays coated with glutamate oxidase and recorded by a FAST recording system (Quanteon, Nicholasville, KY, USA). The slope (nA/μmol/L) and R^2 of microelectrode arrays were calibrated with glutamate-containing solutions before experiments. To measure the extracellular glutamate changes, the tip of the microelectrode arrays was positioned with the glutamate oxidase coating site gently touching the surface of the brain slice. The change of glutamate concentration was calculated by the peak glutamate concentration during SD minus the baseline glutamate concentration. The baseline concentration was calculated by the averaged glutamate concentration during the 2 minutes before high $[K^+]_o$ application. Because microelectrode arrays recording could not be combined with other electrophysiology recordings, all the glutamate measurement experiments were performed with simultaneous IOS imaging to indicate the occurrence of SD onset.

Electrophysiology

Field excitatory postsynaptic potentials (fEPSPs) were evoked by stimulation of the Schaffer collateral pathway of the hippocampus using bipolar tungsten stimulating electrodes and recorded from the CA1 stratum radiatum. Spreading depression-related extracellular direct current potentials were recorded from the cortex or the stratum radiatum of the hippocampus. The fEPSPs and direct current potentials were recorded with glass micropipettes filled with ACSF. Whole-cell currents of cortical L2/3 pyramidal neurons were recorded with glass pipettes filled with Cs-based internal solutions. Field excitatory postsynaptic potentials signals were amplified 1,000 times with an alternating current amplifier (A-M systems, Sequim, WA, USA) and acquired via a Digidata 1440A (Molecular Devices, LLC, Sunnyvale, CA, USA). Direct current potentials and whole-cell currents were monitored with MultiClamp 700B amplifier (Molecular Devices) and acquired via a Digidata 1440A. All data were analyzed with Clampfit 10.0 (Molecular Devices).

Data Analysis

In all bar graphs, values are reported as mean ± standard error of mean (s.e.m.). The gray regions of the averaged traces represent error bars as mean ± s.e.m. connected from each time point. R^2 is the coefficient of determination. Statistical analysis was performed using the Prism statistical analysis program (GraphPad, La Jolla, CA, USA). Normality was tested by D'Agostino–Pearson omnibus test. One-way analysis of variance with Newman–Keuls *post hoc* test was used for statistical comparisons of multiple groups ($>=3$). Two-tailed student's *t*-test was used for statistical comparisons of groups of two. Statistical significance was defined as $^*P<0.05$; $^{**}P<0.01$.

For more details on methodologies, please refer to the Supplementary Information.

RESULTS

Glutamate is Released During Spreading Depression Without Fast Synaptic Transmission

We first determined whether glutamate release still occurred from brain tissue during SD when VGCCs, VGSCs, and evoked synaptic transmission were blocked. In normal ACSF, perfusing high $[K^+]_o$ (40 mmol/L) solution for 90 to 120 seconds consistently triggered SD with a propagation velocity of 5.5 ± 0.3 mm/minute in rat neocortical brain slices (Figure 1A). The SD wave was measured as an extracellular direct current potential shift of approximately 4 mV and a correlated propagating IOS transient, as previously reported (Figure $1B_1$).[8] Using an enzyme-based glutamate electrode positioned within the brain slice, we detected a significant increase in extracellular glutamate during SD, approximately 50 to 100 seconds in duration (peak during SD, 93.2 ± 10.2 μmol/L, $n=7$, Figures $1B_2$ and 1E), within a range consistent with prior work *in vivo*.[12] During the SD wave, this increase of extracellular glutamate temporally coincided with propagation of the IOS component and reached a peak in approximately 5 to 10 seconds (Figure $1B_2$). We then blocked synaptic transmission with Cd^{2+} (30 μmol/L) to inhibit high-threshold VGCCs[13] and tetrodotoxin (TTX, 1 μmol/L) to block VGSCs. Voltage-clamp whole-cell recordings showed that 30 μmol/L of Cd^{2+} was sufficient to completely abolish VGCC-mediated currents in hippocampal neurons (Supplementary Figures 1A, B) and presynaptic Ca^{2+} transients induced by electrical stimuli (Supplementary Figures 1C, D). The effect of Cd^{2+} on synaptic transmission was demonstrated by the complete block of evoked fEPSPs by 30 μmol/L Cd^{2+} ($n=6$, Supplementary Figure 1F). In addition, we blocked action potentials and the presynaptic volley with (TTX, 1 μmol/L, to block VGSCs; Supplementary Figure 1F). Under conditions where VGCCs and VGSCs had been efficiently blocked, SD-like wave propagation was still evoked by perfusing high $[K^+]_o$ solutions, although the glutamate transients were reduced to 52.4 ± 6.3 μmol/L ($n=8$, $P<0.01$ compared with the no-blockers group, Figures 1C and 1D), and propagation rates of SD were reduced to 3.5 ± 0.1 mm/minute (Figure 1H). The amplitudes of extracellular potential shifts and IOS changes during SD were similar in TTX and Cd^{2+} as in control solution suggesting that extracellular glutamate concentrations are still sufficient to saturate glutamate receptors that evoke the postsynaptic depolarization during SD (potentials: 4.39 ± 0.57 mV, $n=6$ in the no-blockers control versus 4.20 ± 0.43 mV, $n=5$ in TTX and Cd^{2+}, $P>0.05$; maximal rate of rise of IOS: 43.6 ± 3.8 ΔT/second, $n=7$ in the no-blockers control versus 52.7 ± 12.6 ΔT/s, $n=7$ in TTX and Cd^{2+}, $P>0.05$; Figures 1E–G). In a subset of experiments we perfused high $[K^+]_o$ in a much higher concentration of Cd^{2+} (200 μmol/L) and 1 μmol/L TTX and still observed a propagating SD with glutamate transients of similar magnitude (41.8 ± 6.5 μmol/L, $n=7$, $P>0.05$ compared within 1 μmol/L TTX and 30 μmol/L Cd^{2+}). These data demonstrate that a large and transient spike of glutamate release occurs during SD, approximately 44% of which is not due to fast synaptic transmission mediated by action potentials and opening of VGCCs. This suggests that although VGCC- and VGSC-dependent processes contribute to glutamate release, when high $[K^+]_o$ is perfused, enough glutamate release can occur via other mechanisms so that

under these conditions, SD propagation does not require action potentials or evoked synaptic transmission. Although the amplitude of the SD waveform did not change we hypothesized that, if SD propagation relies largely on diffusion of glutamate between release sites rather than action potential propagation to presynaptic terminals, then SD propagation rates should be proportional to levels of glutamate release. Plotting the SD propagation rate against the logarithm of glutamate concentrations showed a significant linear correlation ($R^2 = 0.622$, $P < 0.001$, Figure 1I). These results are in accordance with our hypothesis that SD propagation can be mediated by the diffusion of glutamate and when this occurs, glutamate release can occur independent of both action potential propagation and evoked synaptic transmission.

Glutamate is Released by Vesicular Exocytosis but not Transporters or Hemichannels During Spreading Depression

The large component of glutamate release that we still observed after blocking VGCCs and VGSCs with Cd^{2+} and TTX led us to examine whether the glutamate release observed during high $[K^+]_o$-induced SD was due to the exocytosis of glutamate-filled vesicles, or due to other possible non-vesicular mechanisms including glutamate transporters,[14] cystine-glutamate exchangers,[15] and pannexin or connexin hemichannels.[16] We tested the dependence on vesicular exocytosis by examining the effects of bafilomycin A1 and concanamycin A, both of which inhibit vacuolar H^+-ATPase and depress vesicular glutamate release by preventing glutamate transport into synaptic vesicles.[17] To confirm that these inhibitors can block vesicular release of glutamate, we observed that fEPSPs were blocked after slices were treated with either 10 μmol/L bafilomycin alone for >3 hours, or 4 μmol/L bafilomycin or 2 μmol/L concanamycin with brief addition (5 minutes) of 10 μmol/L veratridine to stimulate vesicle turnover.[18] After blockade of fEPSPs with bafilomycin A1 (Figure 2A) or concanamycin A, we applied TTX and Cd^{2+} and evoked SD with perfusion of high $[K^+]_o$ solution. Glutamate release during SD was greatly inhibited by 10 μmol/L bafilomycin (5.2 ± 0.6 μmol/L, $n = 6$, $P < 0.001$), 4 μmol/L bafilomycin plus 10 μmol/L veratridine (2.9 ± 0.5 μmol/L, $n = 6$, $P < 0.001$), or 2 μmol/L concanamycin plus 10 μmol/L veratridine (3.9 ± 1.4 μmol/L, $n = 7$, $P < 0.001$, Figures 2B and 2E). The extracellular potential shifts were also blocked by 10 μmol/L bafilomycin (0.04 ± 0.04 mV, $n = 9$, $P < 0.001$), 4 μmol/L bafilomycin plus 10 μmol/L veratridine (0.0 ± 0.0 mV, $n = 6$, $P < 0.001$), or 2 μmol/L concanamycin plus 10 μmol/L veratridine (0.0 ± 0.0 mV, $n = 6$, $P < 0.001$, Figures 2C and 2F). This indicates that glutamate is released during high $[K^+]_o$-induced SD by a mechanism that requires vesicular exocytosis but is independent of VGCCs and VGSCs. In contrast, none of the inhibitors of the other potential sources of glutamate release exerted any significant reduction on SD-evoked glutamate release (Figure 2G). In fact, DL-*threo*-β-benzyloxyaspartic acid (150 μmol/L), which inhibits both the forward and the reverse operation of glutamate transporters,[19] greatly enhanced both glutamate levels (191.7 ± 37.2 μmol/L, $n = 6$, $P < 0.05$, Figure 2G) and SD propagation rate (5.3 ± 0.3 mm/minute, $n = 4$, $P < 0.01$ compared with control in TTX and Cd, Figure 1H) indicating that function of glutamate transporters during high $[K^+]$-induced SD is to remove glutamate from the extracellular space rather than release via reverse transport. Sulfasalazine (250 μmol/L), an inhibitor of the cystine-glutamate exchanger, which is another potential source of glutamate export,[20] also did not reduce SD-associated glutamate release (48.5 ± 14.6 μmol/L, $n = 6$, $P > 0.05$, Figure 2G). Connexin and pannexin gap junction hemichannels, which allow permeation of molecules <1000 Da, were not involved because the hemichannel blockers mefloquine[21] (selective for pannexins at 0.5 μmol/L)(60.9 ± 13.4 μmol/L, $n = 6$, $P > 0.05$, Figure 2G) and carbenoxolone[22] (effective for both pannexins and connexins at 100 μmol/L)(60.4 ± 5.3 μmol/L, $n = 5$, $P > 0.05$, Figure 2G) failed to inhibit SD-induced glutamate release. These data support vesicular exocytosis as the only source of glutamate release during high $[K^+]_o$-induced SD and suggest glutamate uptake via transporters helps to dampen propagation of this form of SD.

Glutamate Release During Spreading Depression is Dependent Upon NMDARs

Exocytosis of synaptic vesicles at presynaptic sites during synaptic transmission requires elevation of cytosolic Ca^{2+} that results from Ca^{2+} entry via VGCCs.[23] Considering that our results thus far have demonstrated substantial glutamate exocytosis during high $[K^+]_o$-induced SD when synaptic fEPSPs and VGCCs were blocked by Cd^{2+}, we tested for alternative sources of Ca^{2+} entry. NMDARs are permeable to Ca^{2+} and their activation is critical for SD propagation. Recently, it has been reported in several studies that NMDARs are localized to presynaptic terminals and their activation can directly and exclusively promote excitatory neurotransmitter release in the neocortex and hippocampus.[10,11] As such, we hypothesized that when VGCCs, VGSCs, and fEPSPs are blocked, activation of presynaptic NMDARs could still elicit glutamate release during high $[K^+]_o$-induced SD. Accordingly, blockade of NMDARs should not only inhibit SD-induced extracellular potential shifts, which have a substantial component mediated by postsynaptic NMDA glutamate receptors, but also suppress presynaptic vesicular glutamate release. Alternatively, if synaptic release is not dependent upon presynaptic NMDARs, then NMDAR antagonists should only affect postsynaptic depolarization but not the presynaptic glutamate release. We tested this hypothesis by applying NMDAR antagonists D-(-)-2-amino-5-phosphonopentanoic acid (D-APV) (50 μmol/L), 7-chlorokynurenic acid (7-CKA, 100 μmol/L) or MK-801 (10 μmol/L). D-APV and 7-CKA had minimal effect on evoked fEPSPs in the hippocampal slices (Figure 3A), indicating preservation of normal synaptic transmission; however, both glutamate release (1.6 ± 0.4 μmol/L, $n = 8$, $P < 0.001$ with D-APV; 2.1 ± 0.6 μmol/L, $n = 6$, $P < 0.001$ with 7-CKA) and potential shifts (0.0 ± 0.0 mV, $n = 6$, $P < 0.001$ with D-APV or 7-CKA) were abolished during SD (Figures 3B–F). This block was reversible, as the glutamate release was restored in the same slice after D-APV or 7-CKA was washed out (Supplementary Figure 2). An intermediate concentration of D-APV (25 μmol/L) partially reduced glutamate levels (to 26.5 ± 7.5 μmol/L, $n = 4$, $P < 0.05$) and propagation rate (2.7 ± 0.1 mm/minute, $n = 4$, $P < 0.05$, Figures 1H and 1I) in four out of seven slices and completely blocked glutamate release (4.6 ± 1.1 μmol/L, $n = 3$, $P < 0.01$) and SD propagation in the remaining three slices. MK-801 also significantly reduced glutamate release during SD (15.4 ± 4.5 μmol/L, $n = 7$, $P < 0.01$, Supplementary Figure 2). In addition, to exclude the contribution of AMPA and kainate glutamate receptors that are also functionally localized to presynaptic terminals, we tested the AMPA and kainate receptor antagonist 6-cyano-7-nitroquinoxaline-2,3-dione (CNQX) (20 μmol/L) and did not observe any effect on either SD-induced glutamate release (49.7 ± 11.2 μmol/L, $n = 6$, $P > 0.05$, Figure 3E) or potential shifts (5.15 ± 0.42 mV, $n = 4$, $P > 0.05$, Figure 3F). These results suggest that the vesicular glutamate release during high $[K^+]_o$-induced SD is dependent to a significant degree on NMDAR activation, and can occur without the involvement of action potentials, VGCCs, or AMPA/kainate receptors.

To further confirm the NMDAR-dependence of glutamate release, we evoked high $[K^+]_o$-induced SD in solutions containing different concentrations of Mg^{2+}, the voltage-dependent blocker of NMDARs.[24] Mg^{2+} will also differentiate between neuronal NMDARs that are sensitive to extracellular Mg^{2+} and astrocytic NMDARs that are Mg^{2+}-insensitive at concentrations up to 10 mmol/L.[25] Both SD-induced potential shifts and glutamate release were inhibited by Mg^{2+} in a dose-dependent manner with a complete block observed at 5 mmol/L ($n = 6$, Figures 3G and 3H).

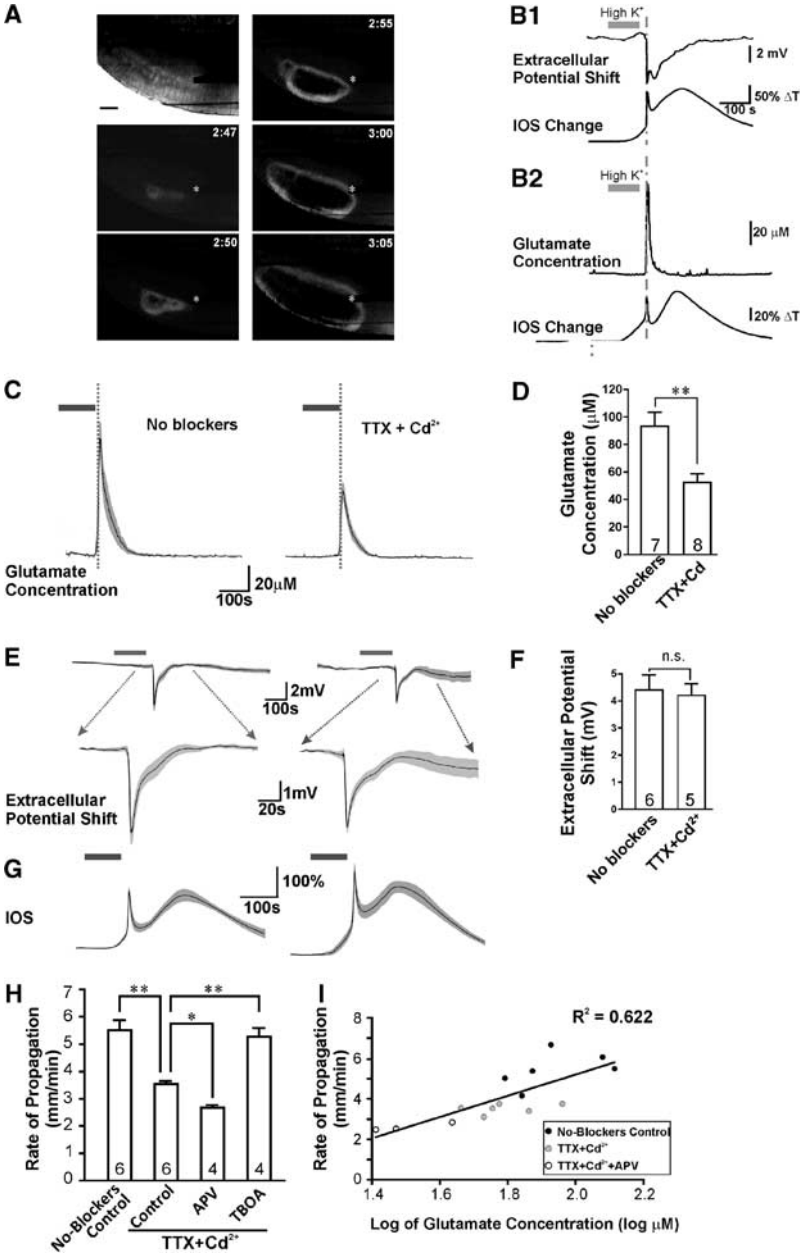

Figure 1. Glutamate transients during spreading depression (SD) were coincident with intrinsic optical signal (IOS) changes and extracellular potential shifts, and occurred independent of action potentials and voltage-gated calcium channels. (**A**) Time series of the IOS difference signal from the same cortical brain slice during the initiation and spread of SD. The left top picture showed the brightfield image of a cortical slice before induction of SD. The propagation of the SD waveform was shown by the change of IOS (at indicated time points (minute:second)) after high $[K^+]_o$ perfusion. The asterisk shows the position of the glutamate enzyme multielectrode array recording site. (**B_1**) The IOS changes were temporally correlated with extracellular potential shifts. (**B_2**) The IOS changes during SD were temporally correlated with glutamate efflux transients. (**C**) Propagating SDs evoked by high $[K^+]_o$ (indicated by the gray bar) were correlated with a large efflux of glutamate that occurred when SD propagated to the site of the glutamate electrode in the neocortex (timing indicated by dotted line). Tetrodotoxin (TTX) and Cd^{2+} partially inhibited the glutamate release. The dashed lines in (**B, C**) indicate the time point when the SD wave front arrived at the recording site. (**D**) Quantification of SD-related glutamate release in control artificial cerebrospinal fluid (ACSF) ($n = 7$ slices from three animals) and ACSF containing TTX and Cd^{2+} ($n = 8$ slices from four animals, by student's *t*-test). (**E**) Traces on the left show high $[K^+]_o$ application (gray bar) triggered SD in the hippocampus as indicated by the extracellular potential shift. Traces on the right demonstrate that the SD extracellular waveforms were not affected by TTX and Cd^{2+}. Dotted arrows indicate regions of the waveforms that are expanded in bottom traces. (**F**) Quantification of SD-related potential shifts in naive slices and slices ($n = 6$ slices from four animals) treated with TTX and Cd^{2+} ($n = 5$ slices from three animals, by student's *t*-test). (**G**) The averaged IOS signals in naive slices and slices treated with TTX and Cd^{2+}. (**H**) The rate of SD propagation in no-blockers solutions ($n = 6$ slices from three animals), control solutions (with 1 μmol/L TTX and 30 μmol/L Cd^{2+}, $n = 6$ slices from three animals), control solutions with 25 μmol/L D-APV ($n = 4$ slices from two animals), and control solutions with 150 μmol/L TBOA ($n = 4$ slices from two animals, by one-way analysis of variance). (**I**) Linear correlative relationship between the logarithm of glutamate concentrations and SD propagation rates from samples of three groups including no-blockers control, TTX, and Cd^{2+}, and medium dose (25 μmol/L) of D-APV that partially inhibits SD-induced glutamate levels. In all figures, experimental values are the mean ± s.e.m. Single asterisk, $P < 0.05$; double asterisk, $P < 0.01$. NS stands for no significance. TBOA, DL-*threo*-β-benzyloxyaspartic acid.

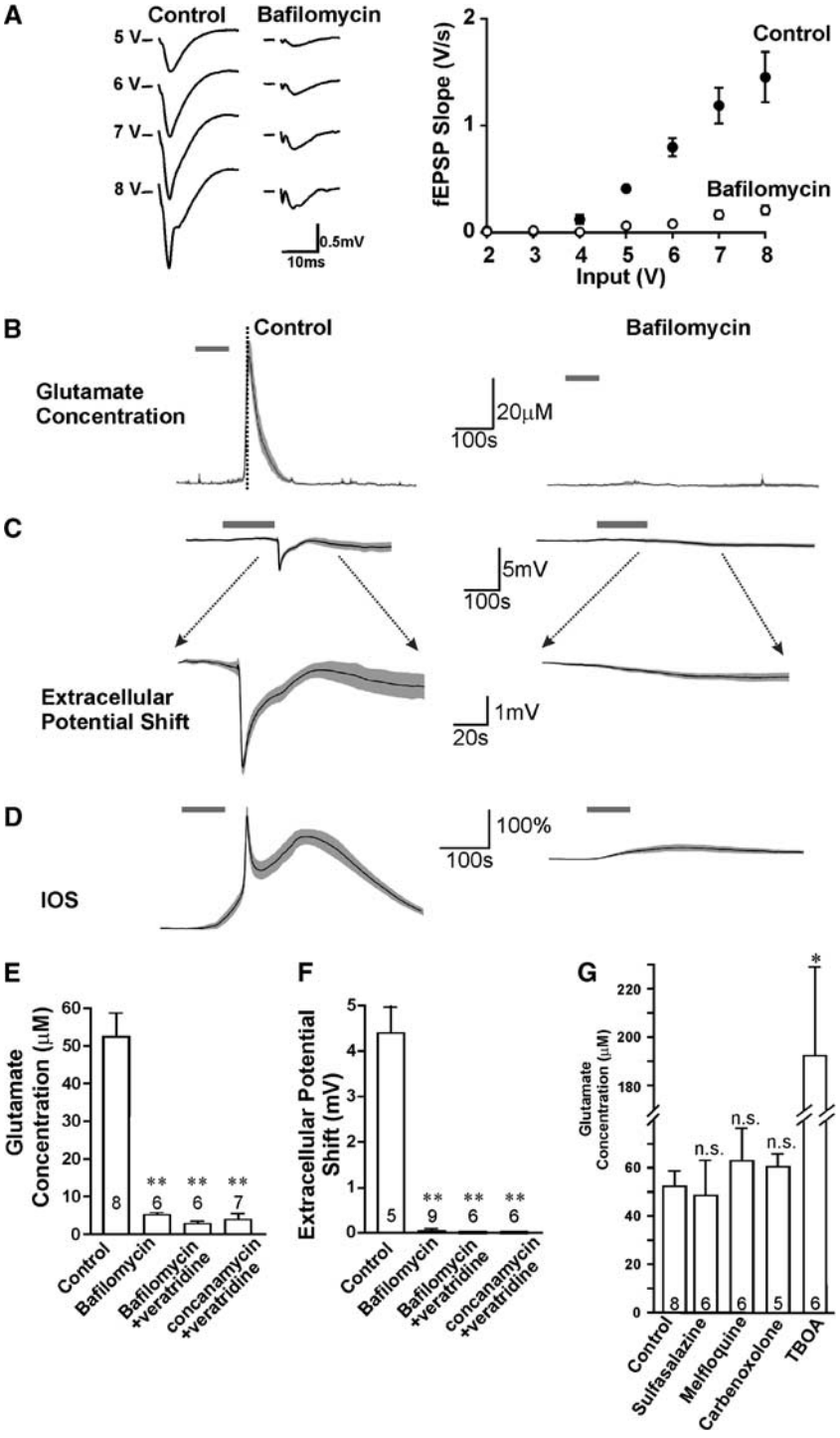

Figure 2. Both the glutamate release and waveforms of spreading depression (SD) required TTX- and Cd^{2+}-insensitive vesicular release. (**A**) Input–output relationship of field excitatory postsynaptic potentials (fEPSP) in control slices and bafilomycin-treated slices in the hippocampus showed that bafilomycin largely inhibited presynaptic transmitter release. (**B**, **C**) Incubating slices in 10 μmol/L bafilomycin for sufficient time to inhibit synaptic transmission blocked SD-induced glutamate release in cortical slices (**B**) and the SD extracellular potential shifts in the hippocampal slices (**C**) as compared with vehicle-treated brain slices. Averaged intrinsic optical signal (IOS) changes from cortical slices were shown in (**D**). Gray bars indicate the high $[K^+]_o$ application. (**E**) Quantification of the glutamate release from control ($n = 8$ slices from four animals), 10 μmol/L bafilomycin alone (>2.5 hours treatment, $n = 6$ slices from two animals), 4 μmol/L bafilomycin plus brief addition of 10 μmol/L veratridine ($n = 6$ slices from two animals), or 2 μmol/L concanamycin plus veratridine ($n = 7$ slices from two animals, by one-way analysis of variance (ANOVA)). (**F**) The extracellular potential shifts showed results from control ($n = 5$ slices from three animals), 10 μmol/L bafilomycin alone (>2.5 hours treatment, $n = 9$ slices from three animals), 4 μmol/L bafilomycin plus brief addition of 10 μmol/L veratridine ($n = 6$ slices from three animals), or 2 μmol/L concanamycin plus veratridine ($n = 6$ slices from three animals, by one-way ANOVA). (**G**) Quantification of glutamate release during SD showing, compared with control slices ($n = 8$ slices from four animals), no reducing effect of TBOA ($n = 6$ slices from two animals), sulfasalazine ($n = 6$ slices from two animals), mefloquine ($n = 6$ slices from two animals) or carbenoxolone ($n = 5$ slices from two animals, by one-way ANOVA). Single asterisk, $P < 0.05$; double asterisk, $P < 0.01$. TBOA, DL-*threo*-β-benzyloxyaspartic acid.

Taken together, these data indicate that the level of glutamate release during high $[K^+]_o$-induced SD is correlated with the extent of NMDAR opening. Moreover, NMDAR-dependent glutamate release from neurons but not astrocytes is critical for SD propagation.

Activation of NMDARs Triggers Vesicular Glutamate Release After Action Potentials and Voltage-Gated Calcium Channels are Blocked

If exocytosis of glutamate-containing vesicles during high $[K^+]_o$-induced SD is directly caused by presynaptic NMDAR opening, we predicted that NMDAR agonists should trigger glutamate release even when synaptic transmission involving action potentials and VGCC-mediated calcium entry is blocked. Consistent with this idea, bath application of 100 μmol/L NMDA in the presence of TTX and Cd^{2+} induced significant glutamate release from brain slices (16.9 ± 1.9 μmol/L, $n = 7$, Figure 3I). Pre-incubation of slices with bafilomycin (4 μmol/L, plus 10 μmol/L veratridine) abolished NMDA-induced glutamate release (0.9 ± 0.4 μmol/L, $n = 6$, $P < 0.01$, Figures 3I and 3J), indicating that the glutamate efflux was vesicular. Considering that NMDAR activation causes glutamate release, and that NMDARs are in turn activated by glutamate, we hypothesized that regenerative NMDAR-dependent gluta-

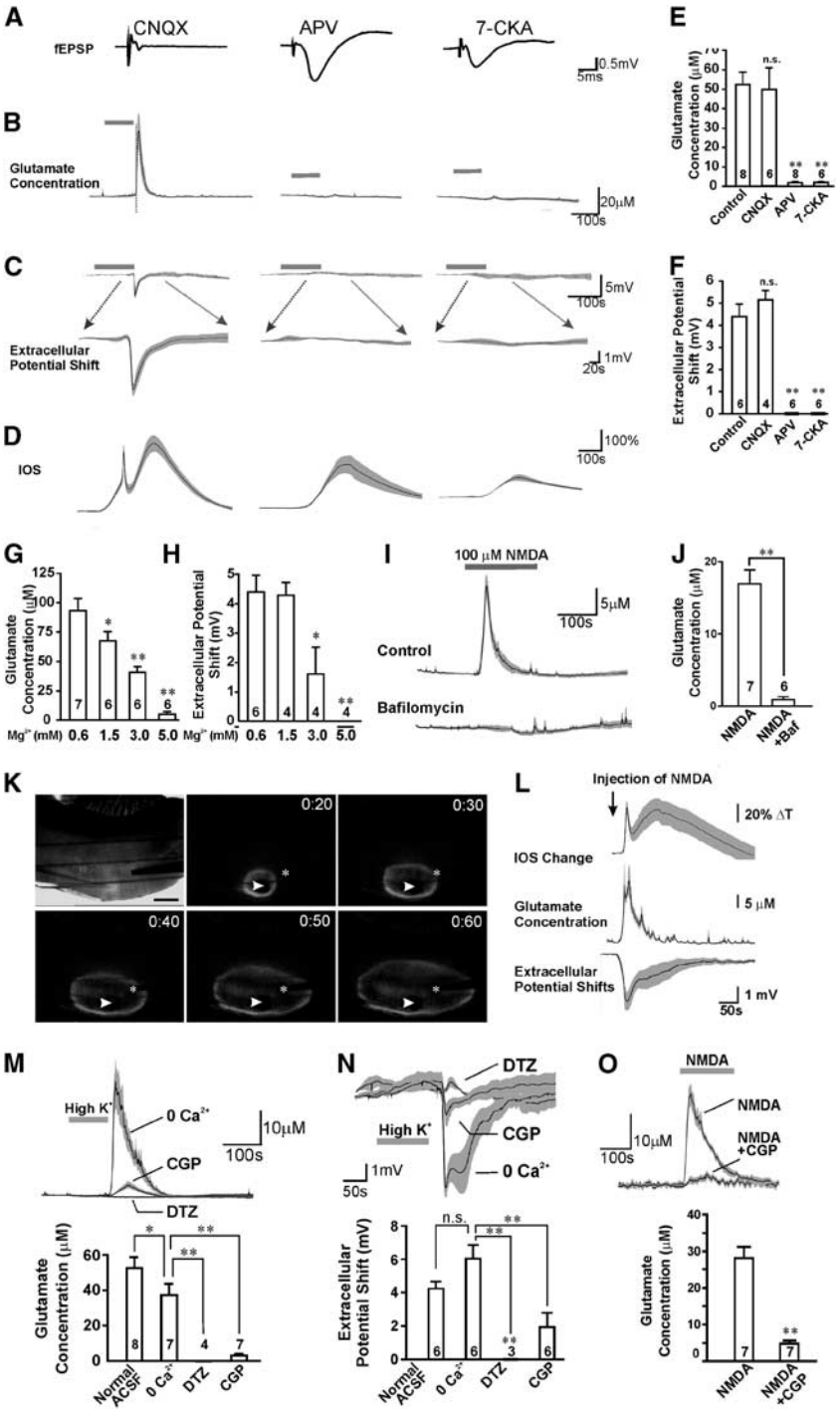

Figure 3. For legend see page 1588.

mate release could be the underlying mechanism of SD wave propagation under these conditions of high $[K^+]_o$. For instance, if extracellular glutamate rose sufficiently as a consequence of NMDAR activation, it could diffuse and activate NMDARs on adjacent synapses, thereby reinitiating the process and triggering a propagating wave. To test this idea, we focally ejected NMDA (500 μmol/L) from a glass pipette onto the surface of brain slices to rapidly activate NMDARs in a given region in the presence of TTX and Cd^{2+}. Notably, we observed that a propagating IOS wave triggered initially at the injection site (at a rate of 1.7 ± 0.2 mm/minute, $n = 6$, Figure 3K) caused transient glutamate release and potential shifts at the wave front (23.5 ± 4.2 μmol/L, $n = 5$; 2.96 ± 0.65 mV, $n = 4$; Figure 3L). This indicates that NMDAR activation under these circumstances is both required and sufficient to evoke an SD-like wave by triggering regenerative glutamate release that is independent of action potential propagation and opening of VGCCs.

NMDA-Dependent Glutamate Release Involves Both Ca^{2+} Influx and Activation of the Mitochondrial Na^+/Ca^{2+} Exchanger (NCX_{mito})

NMDAR activation may induce glutamate release either by directly producing a calcium influx across cell membranes, or by activating secondary calcium-permeable channels or transporters close to the vesicle release sites. To test the contribution of calcium influx, we examined whether we could induce SD by applying high $[K^+]_o$ in solutions containing 0 mmol/L extracellular Ca^{2+} with 2 mmol/L EGTA (0 $[Ca^{2+}]_o$ solution) in the presence of TTX and Cd^{2+}. Surprisingly, we still observed propagating SD that occurred concurrently with a transient, albeit decreased, glutamate release (37.3 ± 6.7 μmol/L, $n = 7$, $P < 0.05$ compared with normal ACSF with TTX and Cd^{2+}, Figure 3M; potential shift 5.99 ± 0.83 mV, $n = 6$, Figure 3N). These data indicate that Ca^{2+} influx partially contributes to glutamate release. We investigated further the substantial glutamate release in 0 $[Ca^{2+}]_o$ solutions, because this suggests that release of Ca^{2+} from intracellular stores can also contribute to evoking glutamate release during high $[K^+]_o$-induced SD. NMDARs are permeable to Na^+ in addition to Ca^{2+} and intense receptor activation would increase intracellular Na^+ ($[Na^+]_i$) and possibly induce Ca^{2+} efflux from mitochondria via the Na^+/Ca^{2+} exchangers (NCX_{mito}) as described previously.[26] Mitochondria are typically found in presynaptic terminals adjacent to synaptic vesicles at active zones[27] and previous studies have shown that substantial neurotransmitter release occurs when increased cytosolic Na^+ triggers NCX_{mito} dependent Ca^{2+} release from mitochondria in presynaptic terminals.[28] To investigate the involvement of NCX_{mito}, we tested the effect of CGP-37157 (CGP, 7-chloro-5-(2-chlorophenyl)-1,5-dihydro-4,1-benzothiazepin-2(3H)-one), which is a specific NCX_{mito} blocker,[29] on SD-induced glutamate release under the conditions of 0 $[Ca^{2+}]_o$ solutions containing TTX and Cd^{2+}. CGP-37157 (20 μmol/L), inhibited both SD-induced glutamate transients (3.1 ± 1.1 μmol/L, $n = 7$, $P < 0.05$, Figure 3M) and SD potential shifts (1.93 ± 0.87 mV, $n = 6$, $P < 0.01$, Figure 3N), supporting a significant role for NCX_{mito} in the glutamate release during SD. The less selective but also potent NCX_{mito} blocker diltiazem (500 μmol/L) abolished both the SD-induced glutamate release (0.0 ± 0.0, $n = 4$, $P < 0.01$) and the potential shifts (0.0 ± 0.0, $n = 3$, $P < 0.01$, Figures 3M and 3N). Although diltiazem also depresses L-type Ca^{2+} channels at high concentrations, this should not be a factor because the solutions contained Cd^{2+} at concentrations that are sufficient to inhibit L-type calcium channels.[13] Next, we examined whether NMDAR activation in the absence of Ca^{2+} entry could trigger glutamate release by NCX_{mito} activation, by bath applying NMDA (100 μmol/L) in 0 $[Ca^{2+}]_o$ ACSF containing TTX and Cd^{2+}. Even in 0 $[Ca^{2+}]_o$, NMDA still evoked glutamate release from brain slices (28.0 ± 3.1 μmol/L, $n = 7$, Figure 3O) which was significantly inhibited by CGP-37157 (4.7 ± 0.8 μmol/L, $n = 7$, $P < 0.001$). Taken together, these data suggest that glutamate release during high $[K^+]_o$-induced SD is dependent upon both Ca^{2+} influx from NMDAR activation and Ca^{2+} release from mitochondria via NCX_{mito}.

Presynaptic NMDARs are Activated During Spreading Depression

From the results above, we inferred that a significant component of glutamate release during high $[K^+]_o$-induced SD is caused by activation of presynaptic NMDARs. Several studies have employed electrophysiological recordings of minitature excitatory postsynaptic currents (mEPSCs) to demonstrate the facilitatory effect of presynaptic NMDARs on spontaneous neurotransmitter release.[11] In these studies, using cortical neurons where postsynaptic

Figure 3. Activation of *N*-methyl-D-aspartate receptors (NMDARs) was required and sufficient for glutamate release and spreading depression (SD)-like waves. (**A**) CNQX, the AMPA/kainate receptor antagonist, but not D-APV, the NMDAR antagonist, abolished evoked field excitatory postsynaptic potentials (fEPSPs) in hippocampal slices. After tetrodotoxin and Cd^{2+} were perfused to block action potentials and calcium channels, CNQX had no effect on cortical glutamate release during SD (**B**) or on the hippocampal SD waveform (**C**) whereas APV and 7-CKA blocked both the glutamate release and SD waveform. (**D**) The averaged IOS changes in cortical slices. High $[K^+]_o$ application is indicated as the gray bar. (**E**) Quantification of the SD-induced glutamate release in CNQX ($n = 6$ slices from two animals), APV ($n = 8$ slices from four animals), and 7-CKA ($n = 6$ slices from two animals). (**F**) Extracellular potentials in CNQX ($n = 4$ slices from 2 animals), APV ($n = 6$ slices from 2 animals), and 7-CKA ($n = 6$ slices from two animals). (**G**) Spreading depression-induced glutamate release was blocked in a dose-dependent manner by 0.6 mmol/L ($n = 7$ slices from three animals), 1.5 mmol/L ($n = 6$ slices from two animals), 3.0 mmol/L ($n = 6$ slices from two animals), and 5.0 $[Mg^{2+}]_o$ ($n = 6$ slices from two animals) in cortical slices. (**H**) Extracellular potential shifts were blocked by 0.6 mmol/L ($n = 6$ slices from three animals), 1.5 mmol/L ($n = 4$ slices from two animals), 3.0 mmol/L ($n = 4$ slices from two animals), and 5.0 $[Mg^{2+}]_o$ ($n = 4$ slices from two animals, by one-way analysis of variance (ANOVA)) in hippocampal slices. (**I**, **J**) Bath application of 100 μmol/L NMDA induced glutamate release ($n = 7$ slices from three animals) in the presence of TTX and Cd^{2+} in the cortex, but this glutamate release was blocked by pretreatment with 4 μmol/L bafilomycin ($n = 6$ slices from one animal, by student's *t*-test). (**K**) Focal application of 500 μmol/L NMDA induced a SD-like wave of intrinsic optical signal (IOS) in the presence of TTX and Cd^{2+}. The top left image shows the IOS of a cortical slice before NMDA application. The other images show SD propagation indicated by IOS signals (at indicated time points (minute:second)) after NMDA ejection at 0:00. The white arrow and asterisk show the sites of the ejection pipette tip and the glutamate sensor, respectively. Scale bar, 0.5 mm. (**L**) Focal ejection of NMDA induced a glutamate transient and extracellular potential shifts that were coincident with IOS signals. (**M**) The high $[K^+]_o$-induced transient glutamate release still occurred when extracellular Ca^{2+} was removed (0 $[Ca^{2+}]_o$) with TTX and Cd^{2+} ($n = 7$ slices from four animals) as compared with normal artificial cerebrospinal fluid (ACSF) with TTX and Cd^{2+}. Blocking NCX_{mito} with either diltiazem (DTZ) ($n = 4$ slices from two animals) or CGP ($n = 7$ slices from three animals) significantly reduced glutamate release in 0 $[Ca^{2+}]_o$ solutions containing TTX and Cd^{2+}. (**N**) Under the same conditions as in panel **M**, DTZ ($n = 3$ slices from one animal) and CGP ($n = 6$ slices from three animals) both significantly inhibited the hippocampal potential shifts of SD as compare to control in 0 $[Ca^{2+}]_o$ solutions ($n = 6$ slices from three animals, by one-way ANOVA). (**O**) Bath application of 100 μmol/L NMDA in 0 $[Ca^{2+}]_o$ solutions with TTX and Cd^{2+} induced glutamate release ($n = 7$ slices from two animals), which was blocked by 20 μmol/L CGP ($n = 7$ slices from two animals, by student's *t*-test). Single asterisk, $P < 0.05$; double asterisk, $P < 0.01$. CGP, 7-chloro-5-(2-chlorophenyl)-1,5-dihydro-4,1-benzothiazepin-2(3H)-one; CNQX, 6-cyano-7-nitroquinoxaline-2,3-dione.

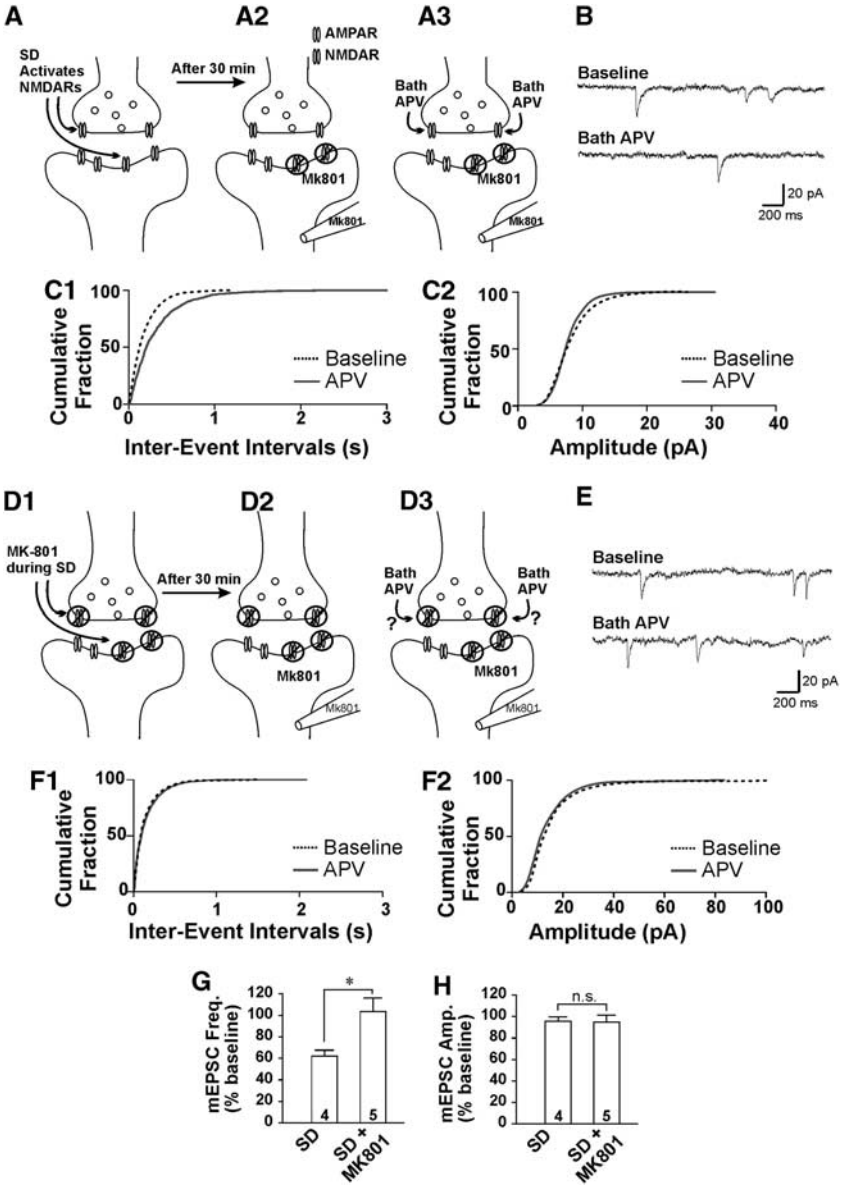

Figure 4. Activation of presynaptic *N*-methyl-D-aspartate receptors (NMDARs) during spreading depression (SD). (**A**) Illustration showing how to examine presynaptic NMDAR components by recording mEPSCs after postsynaptic NMDARs are blocked. (**A_1**) SD was induced in the neocortical slices. (**A_2**) 30 minutes after SD induction, whole-cell recordings were performed in L2/3 neurons. (**A_3**), D-APV was bath-applied after a stable baseline of mEPSCs was recorded. (**B**) Sample traces showing mEPSCs before and 5 minutes after washing-in of D-APV during blockade of postsynaptic NMDARs in cortical L2/3 pyramidal neurons. (**C**) Cumulative probability histograms showed that D-APV decreased the frequency (**C_1**) but not amplitude of mEPSCs (**C_2**) from the same neuron in panel **B**. (**D**) Illustration showing that MK-801 application during SD induction blocks presynaptic NMDARs (**D_1**). mEPSCs were recorded 30 min after SD induction and wash-out of MK-801. (**D_2**) MK-801 occluded the effects of subsequent D-APV application on mEPSCs (**D_3**). (**E**) Sample traces showing mEPSCs before and 5 minutes after washing-in of D-APV during blockade of postsynaptic NMDARs in slices in which SD was previously induced in the presence of MK-801. (**F**) Cumulative probability histograms showed that D-APV did not alter either the frequency (**F_1**) or amplitude (**F_2**) of mEPSCs from the same neuron in panel **E**. (**G**) D-APV significantly decreased mEPSC frequency in slices in which SD was previously induced under control conditions, but this effect was occluded by the MK-801 treatment during SD. (**H**) D-APV did not change mEPSC amplitude in slices in which SD was previously induced either under control conditions or with MK-801. In panels **G** and **H** mEPSCs were collected and analyzed from 300-second recordings, and were normalized to their respective baselines before washing-in of D-APV (SD: $n = 4$ slices from three animals; $n = 5$ slices from five animals, by Student's *t*-test). Single asterisk, $P < 0.05$. mEPSC, minitature excitatory postsynaptic current.

NMDARs were blocked, the NMDAR antagonist D-APV decreased the frequency but not the amplitude of mEPSCs. We investigated whether presynaptic NMDARs were indeed activated during SD by applying MK-801 during SD induction. MK-801 is an irreversible, open channel blocker of NMDARs, and will only block channels that are activated during SD. We predicted that if presynaptic NMDARs were stimulated during SD then MK-801 would occlude the effects of a subsequent D-APV application on decreasing the frequency of mEPSCs. In our experiments, postsynaptic NMDARs were first blocked by inclusion of MK-801 (1 mmol/L) in the intracellular recording solution (Figure $4A_2$), and the effects of presynaptic NMDAR block on mEPSCs were tested by subsequently applying D-APV (Figure $4A_3$). In control slices with no MK-801 added during SD, mEPSCs were recorded in cortical layer

2/3 pyramidal neurons 30 minutes after SD was induced (Figure $4A_1$) to ensure that SD itself did not obscure presynaptic actions of NMDAR activation. Consistent with previous studies, D-APV (100 μmol/L) significantly reduced the frequency of mEPSCs ($62.1 \pm 5.5\%$ of baseline, $n = 4$, Figure 4B, C_1, G) but did not affect the amplitude ($95.6 \pm 4.0\%$, $n = 4$, Figures 4B, $4C_2$, and 4H), indicating a presynaptic regulatory function of NMDARs. If our hypothesis that presynaptic NMDARs are activated during SD is correct, then exposure to MK-801 during SD will irreversibly block presynaptic NMDARs during SD (Figure $4D_1$) and this will occlude the depression of mEPSC frequency by D-APV when tested after SD (Figures $4D_2$ and $4D_3$). When D-APV was bath-applied after MK-801 (20 μmol/L) was present during SD and unbound MK-801 was washed out for 30 minutes after SD, we found that D-APV had no effect on either the frequency ($103.7 \pm 12.3\%$, $n = 5$, $P < 0.05$ compared with SD, Figures 4E, $4F_1$, and 4G) or the amplitude of mEPSCs ($95.0 \pm 6.2\%$, $n = 5$, $P = 0.95$ compared with SD; Figures 4E, $4F_2$ and 4H). This suggests that the effect of D-APV on presynaptic NMDARs is occluded by the previous application of MK-801 during SD, and strongly indicates that presynaptic NMDARs are activated during SD induction and propagation.

Glutamate Release During Spreading Depression Requires Presynaptic NMDARs

The requirement of presynaptic versus postsynaptic NMDAR activation for eliciting glutamate release during SD was further investigated using a strategy to block either post- or presynaptic NMDARs pharmacologically before evoking SD. We designed two strategies to selectively depolarize either presynaptic terminals or postsynaptic dendrites with co-application of MK-801 to selectively and irreversibly block NMDARs at either site. The first strategy to selectively stimulate and block postsynaptic NMDARs was as follows: presynaptic release was inhibited by baclofen (to activate $GABA_B$ receptors) in addition to blocking action potentials with TTX, and VGCCs with Cd^{2+}. In addition, NMDAR channel activity at resting membrane potentials was decreased with higher extracellular Mg^{2+} (1 mol/L). Therefore, we used 1 μmol/L TTX, 30 μmol/L Cd^{2+}, and 10 μmol/L baclofen to inhibit presynaptic depolarization, together with 1 μmol/L AMPA to depolarize postsynaptic dendrites and 10 μmol/L MK-801 to irreversibly block postsynaptic NMDARs when they are activated by spontaneous glutamate release (Figure 5A, Supplementary Figures 3A, B). We also confirmed that the combined treatment did not affect presynaptic NMDARs as shown by blocking NMDARs with D-APV on mEPSCs recordings with intracellular MK-801 (Supplementary Figure 4). As the combination of TTX, Cd^{2+}, baclofen, AMPA, and MK-801 only blocked postsynaptic NMDARs and did not affect presynaptic NMDARs, we used this treatment to examine whether blockade of postsynaptic NMDARs would impair SD. Blocking postsynaptic NMDARs significantly reduced the extracellular potential shifts (2.40 ± 0.30 mV, $n = 6$, versus 5.93 ± 0.40 mV, $n = 6$ in control slices, $P < 0.01$, Figures 5C and 5E), indicating that postsynaptic NMDA receptors contribute substantially to the membrane depolarization that accompanies SD propagation. However, glutamate release during SD was not significantly affected (59.98 ± 6.52 μmol/L, $n = 7$ versus 64.43 ± 10.38 μmol/L, $n = 7$ in control, $P > 0.05$, Figures 5B and 5D), and the propagating rate of SD was not significantly different from control slices (3.5 ± 0.3 mm/minute, $n = 6$, compared with 3.8 ± 0.2 mm/minute, $n = 6$, $P > 0.05$ in control). These results suggest that postsynaptic NMDARs are not responsible for evoking the glutamate release during SD, but instead contribute to the postsynaptic neuronal depolarization.

The second strategy was aimed to block presynaptic NMDARs by stimulating presynaptic terminals in the presence of MK-801. We used CNQX to inhibit postsynaptic activities, together with nicotine to depolarize presynaptic compartments and MK-801 to irreversibly block presynaptic NMDARs activated by spontaneous glutamate release stimulated by the presynaptic actions of

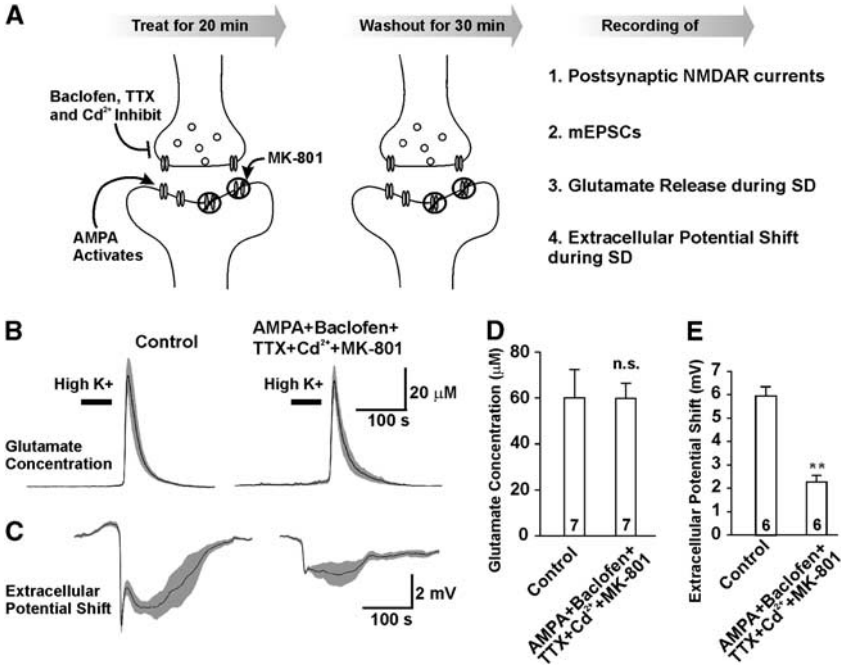

Figure 5. Postsynaptic *N*-methyl-D-aspartate receptors (NMDARs) were not required for glutamate release during spreading depression (SD). (**A**) Illustration of experimental procedures to pharmacologically block postsynaptic NMDARs in neocortex by 1 μmol/L, tetrodotoxin (TTX), 30 μM Cd^{2+}, 10 μmol/L baclofen, 1 μmol/L AMPA and 10 μmol/L MK-801, followed by 30 minute wash. (**B, C**) The combined treatment did not change glutamate release (**B**) but reduced extracellular potential shifts of SD (**C**). (**D**) Summary of glutamate release ($n = 7$ slices from four animals in control and $n = 7$ slices from two animals in cocktail treatment). (**E**) Summary of extracellular potential shifts ($n = 6$ slices from four animals in control and $n = 6$ slices from two animals in cocktail treatment). Student's *t*-test; single asterisk, $P < 0.05$; double asterisk, $P < 0.01$.

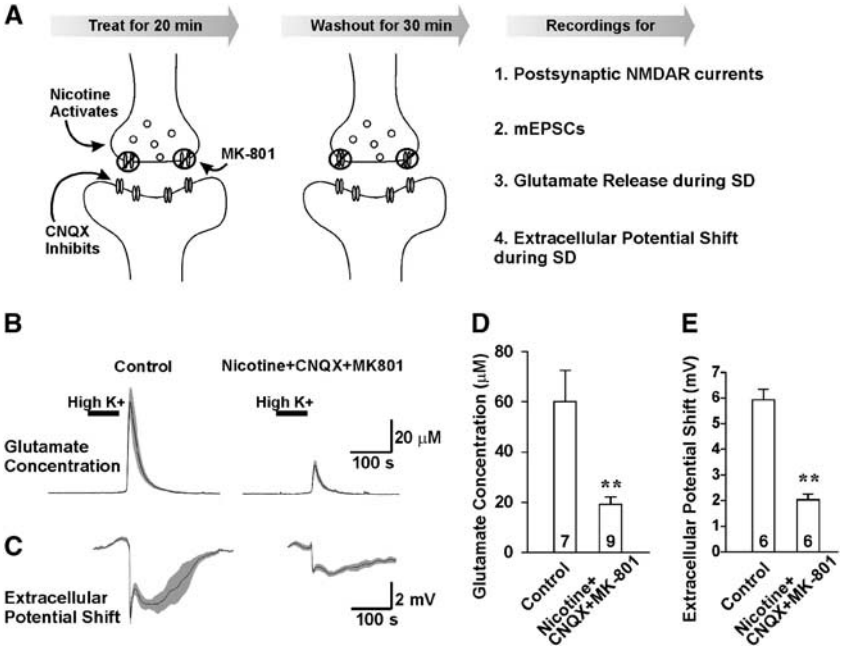

Figure 6. Blocking presynaptic *N*-methyl-D-aspartate receptors (NMDARs) inhibited glutamate release during spreading depression (SD). (**A**) Illustration showing pharmacological blockade of presynaptic NMDARs in neocortex by the combined treatment of 20 μmol/l CNQX, 1 μmol/L nicotine, and 10 μmol/l MK-801 followed by 30 minute wash. (**B**, **C**) MK-801, nicotine, and CNQX decreased both glutamate release (**B**) and extracellular potential shifts of SD (**C**). (**D**) Summary of glutamate release ($n = 7$ slices from four animals in control and $n = 9$ slices from three animals in cocktail treatment). (**E**) Summary of extracellular potential shifts ($n = 6$ slices from four animals in control and $n = 6$ slices from two animals in cocktail treatment). Student's *t*-test; double asterisk, $P < 0.01$. CNQX, 6-cyano-7-nitroquinoxaline-2,3-dione.

nicotine (Figure 6A). These manipulations would reduce postsynaptic depolarization, thereby decreasing the ability of MK-801 to block postsynaptic NMDARs and increase its ability to block presynaptic NMDARs. The slices were treated with the combination of 20 μmol/L CNQX, 1 μmol/L nicotine, and 10 μmol/L MK-801 for 20 minutes followed by a 30-minute wash. Our results showed that the postsynaptic NMDAR currents were not significantly affected (Supplementary Figures 3C, D). Instead, the presynaptic NMDAR components were inhibited by the combined treatment (Supplementary Figure 4). After specifically blocking pre- but not postsynaptic NMDARs, glutamate release was significantly reduced (19.29 ± 2.85 μmol/L, $n = 9$, $P < 0.01$, Figures 6B and 6D), and the extracellular potential shifts were also inhibited (2.03 ± 0.21 mV, $n = 6$, $P < 0.01$, Figures 6C and 6E). In addition, the propagating rate of SD was reduced to 2.4 ± 0.2 mm/minute ($n = 6$, $P < 0.01$ compared with control). These data demonstrate that presynaptic but not postsynaptic NMDARs are required for glutamate release, and that this form of glutamate release is causally related to SD progression in the neocortex.

NMDA Triggers Propagating Spreading Depression and Glutamate Release in the Striatum That Lacks Glutamatergic Neurons

Our results in the cortex suggest that presynaptic NMDARs are required for the regenerative glutamate release in high $[K^+]_o$-induced SD that occurs when action potentials are blocked by TTX and VGCCs are blocked by Cd^{2+}. It is still possible that the substantial postsynaptic dendritic depolarization of glutamatergic cortical neurons could passively depolarize presynaptic terminals of recurrent collaterals and thereby contribute to glutamate release. We performed experiments in another brain region to test whether NMDAR actions on presynaptic terminals were sufficient to trigger SD-induced glutamate release where there was no possible contribution from neuronal depolarization and subsequent passive depolarization of axons and presynaptic terminals to activate calcium influx at distal sites. We investigated glutamate release during SD in the isolated striatal brain slices that lack glutamatergic cell bodies but only contain glutamatergic presynaptic terminals from neocortical projections to the principal GABAergic striatal neurons.[30] NMDAR-dependent glutamate release during SD propagation in this tissue would only be from glutamate diffusion between adjacent terminals and could not be due to passive propagation of postsynaptic depolarizations to presynaptic terminals. We repeated our SD experiments with focal NMDA application in isolated striatal slices where surrounding regions such as neocortex and the septal area were carefully removed (Figure 7A). We found that in the presence of 1 μmol/L TTX and 30 μmol/L Cd^{2+}, focal ejection of 500 μmol/L NMDA from a glass pipette evoked a SD-like waveform that propagated at a rate of 1.9 ± 0.2 mm/minute from the initiation site (indicated by arrow head, $n = 6$, Figure 7A). The wave front of the IOS changes was temporally coincident with both transient glutamate increase (58.5 ± 15.4 μmol/L, $n = 4$, Figures 7B and 7D) and extracellular potential shift (2.37 ± 0.28 mV, $n = 5$, recording location indicated by the asterisk, Figure 7C), which were both blocked by 50 μmol/L of APV (0 ± 0 μmol/L, $n = 2$, $P < 0.05$ and 0 ± 0 mV, $n = 3$, $P < 0.05$). These results show that SD is able to propagate in a brain region containing no recurrent glutamatergic connections but rather purely presynaptic endings, likely by a mechanism involving the diffusion of glutamate that is released by activation of presynaptic NMDARs.

DISCUSSION

In this study, we show that an unusual form of regenerative glutamate release that occurs during high $[K^+]_o$-induced SD is sufficient for SD propagation. We conclude that presynaptic NMDARs are required for this regenerative glutamate release because: (1) glutamate release during SD was blocked by NMDAR antagonists but not by inhibiting pannexins, connexins, AMPA/

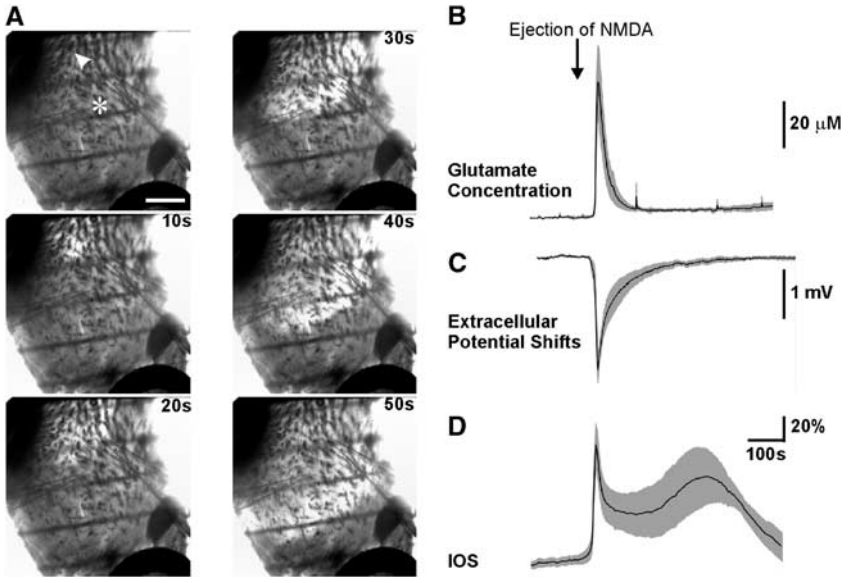

Figure 7. *N*-methyl-D-aspartate NMDA induced spreading depression-like waves in striatal slices. (**A**) The brightfield image of a striatal slice before and during induction of SD by focal ejection of 500 μmol/L NMDA in tetrodotoxin and Cd^{2+} (30 μmol/L). The arrow and asterisk indicate the position of the puffing electrode and the recording electrode respectively. The propagation of SD-like waveform was shown by the change of intrinsic optical signals at indicated time points (seconds) after the transient NMDA ejection. Scale bar, 0.5 mm. *N*-methyl-D-aspartate ejection evoked glutamate efflux transients (**B**, $n = 4$ slices from two animals), extracellular potential shifts (**C,** $n = 5$ slices from 2 animals), and IOS changes (**D**) in striatal slices.

kainate receptors, glutamate transporters, cystine-glutamate exchangers, VGSCs or VGCCs; (2) NMDAR-dependent glutamate release during SD requires vesicular exocytosis, as it is sensitive to bafilomycin and concanamycin; (3) when VGSCs and VGCCs were blocked, directly applying NMDA itself still induced bafilomycin-sensitive glutamate release that could trigger SD wave propagation in neocortical and striatal slices. In addition, our strategy to selectively inhibit presynaptic NMDARs dramatically reduced glutamate release during high $[K^+]_o$ SD whereas selectively blocking postsynaptic glutamate receptors had no effect on glutamate release. Our data indicate that regenerative glutamate release during high $[K^+]_o$-induced SD can occur independently of canonical fast transmission across synapses that requires action potential invasion in presynaptic terminals and calcium influx through VGCCs. In contrast, our evidence indicates that a substantial fraction of glutamate release during SD triggered by high $[K^+]_o$ requires opening of presynaptic NMDARs that induces vesicular exocytosis of glutamate. We propose that during high $[K^+]_o$-induced SD glutamate can diffuse to adjacent synapses to activate more NMDARs and trigger a self-propagating regenerative process that underlies the propagation of this form of SD.

Previous studies have shown that both SD initiation and propagation are inhibited by NMDAR antagonists. Although NMDARs are more abundantly distributed at postsynaptic sites, the ability of NMDA to evoke glutamate release in the presence of VGCC and VGSC antagonists, which blocked evoked fEPSPs, argues against postsynaptic depolarization triggering action potential propagation from soma to axon terminals. Our observations that SD propagates in the isolated striatum, where there are no glutamatergic cell bodies only presynaptic terminals, indicate that glutamate release is not due to passive propagation of postsynaptic depolarizations in glutamatergic neurons causing release from presynaptic terminals. Although dendritic release of glutamate can occur from olfactory mitral cells,[31] it is unlikely that our observations are due to such a mechanism, because dendritic glutamate release requires specialized dendrodendritic interactions and dendritic glutamate-containing vesicles but neither of these morphologies has been observed in the cortex or hippocampus.[32] The simplest explanation, in light of the high levels of functional expression of NMDARs in axons and presynaptic terminals in the cortex and hippocampus, is that NMDA acting on receptors on presynaptic axons and terminals is sufficient for the release of glutamate-containing vesicles. The enhanced release of vesicles from terminals could also explain the observed release of other SD-related neurochemicals like zinc that are found in vesicles.[5] Our results also suggest that both Ca^{2+} and Na^+ influx via NMDARs is important for this process as Ca^{2+} release from mitochondria can have a role through the action of NCX_{mito}. Mitochondria are typically found at metabolically active presynaptic terminals[27,33] and are increasingly recognized as important for buffering and releasing calcium in neurons and at synapses.[34,35] At present, because of the dramatic swelling and subsequent movement of all presynaptic and dendritic cellular components that occurs rapidly at the onset of SD as previously reported,[8] we are unable to track mitochondrial Ca^{2+} signals in presynaptic terminals during SD. Nevertheless, the role for Ca^{2+} release via NCX_{mito} is indicated by our data that both SD- and NMDA-induced glutamate releases were inhibited by the selective NCX_{mito} blocker CGP-37157 and by diltiazem when extracellular Ca^{2+} was removed. The presynaptic role of NMDARs is further demonstrated by our findings that presynaptic NMDARs are indeed activated during high $[K^+]_o$ SD, and that blocking presynaptic NMDARs reduces glutamate release. Activation of presynaptic NMDARs was tested by the irreversible, use-dependent NMDAR blocker MK-801. When MK-801 was applied during SD to block NMDAR activated during SD, we no longer observed a decrease in mEPSC frequency by the NMDAR antagonist D-APV indicating that the facilitative effects of presynaptic NMDARs on neurotransmitter release were occluded. Using MK-801 to block NMDARs at specific synaptic locations also suggests that only presynaptic receptors are required for glutamate release, and that postsynaptic NMDARs partially contribute to the slow potential shifts. These results strongly suggest that presynaptic NMDAR-mediated glutamate release is a critical step in the positive feedback cycle required for SD propagation triggered by high $[K^+]_o$.

Our observations that SD propagation rates are linearly correlated with the logarithm of glutamate concentrations indicate that SD depends on diffusion of glutamate between release sites rather than action potential propagation between synaptic connections. Mechanisms that increase glutamate release at synapses will accelerate propagation speed by both increasing concentration gradients and by activating more presynaptic NMDARs thereby facilitating the regenerative glutamate release. In line with this speculation, our prior work has demonstrated that glutamate release through volume-activated channels in astrocytes contributes to the propagation of SD, suggesting that such a mechanism might be important in facilitating glutamate diffusion in at least some forms of SD.[36] The present study shows that other known mechanisms of astrocytic and neuronal glutamate release are not likely involved, including hemichannels, P2X7 receptor channels, reversed operation of glutamate transporters, or cystine-glutamate antiporters.[37] Our data that Mg^{2+} dose-dependently inhibited glutamate release also suggest that NMDAR-dependent glutamate release is from neurons rather than astrocytes.

Prolonged increases of extracellular K^+ levels have been observed after several pathologic conditions, like subarachnoid hemorrhage, intracerebral hemorrhage, and traumatic brain injury,[38–40] and may contribute to SD incidence under these conditions. Raised $[K^+]_o$ will inhibit or reverse glutamate transporters and reduce the efficiency of glutamate uptake, which might facilitate spillover of glutamate from the synaptic release sites and increase the diffusion.[41] The shrinkage of interstitial space caused by raising $[K^+]_o$ will also increase the concentrations of extracellular glutamate. Elevated $[K^+]_o$ can also depolarize presynaptic terminals and remove the Mg^{2+} blockade of presynaptic NMDA receptors. These multiple factors could all contribute to maintain the positive feedback cycle of presynaptic NMDAR activation during SD. This is in line with a previous study where the threshold of SD triggered by high $[K^+]_o$ was increased by NMDAR antagonists.[42]

Brief focal application of a small volume of high $[K^+]_o$ to cortical surfaces *in vivo* or to cortical slices under physiologic conditions induces SD that is sensitive to VGCC blockers or extracellular Ca^{2+} removal.[5,6] The mutant mice with loss-of-function P/Q VGCC displayed 10-fold higher threshold than controls when SD was induced by brief focal K^+ application or electrical stimuli.[43] Interestingly, knock-in mice carrying the *familial hemiplegic migraine type 1* gene, a mutant P/Q-type VGCC with a gain-of-function phenotype, exhibit increased probability of glutamate release, lower SD threshold, and increased SD propagation velocity.[44] It is possible that the P/Q channel-dependent SD involves different or additional mechanisms than those we observed during high $[K^+]_o$-triggered SD. However further studies are needed to define the relative contribution of presynaptic NMDARs to SD events under different conditions *in vivo*.

The incidence of SD in the human cortex is highly correlated with exacerbation of brain damage after malignant hemispheric stroke, delayed ischemia induced by subarachnoid hemorrhage, intracranial hemorrhage, and traumatic brain injury.[1,2] Blocking SD by NMDAR antagonists was observed to be neuroprotective after brain injury in clinical studies.[45] Our study reveals that a novel form of presynaptic NMDAR-dependent regenerative glutamate release that is independent of VGSC and VGCC activation contributes to and in some circumstances is sufficient for SD propagation. Such a mechanism may explain how SD propagates in the 'isoelectric' brain when typical synaptic transmission through action potential propagation is already suppressed.[46] It is possible that selectively targeting antagonists against presynaptic NMDARs could reduce SD-related neurologic conditions.

DISCLOSURE/CONFLICT OF INTEREST

The authors declare no conflict of interest.

REFERENCES

1 Dreier JP. The role of spreading depression, spreading depolarization and spreading ischemia in neurological disease. *Nat Med* 2011; **17**: 439–447.
2 Lauritzen M, Dreier JP, Fabricius M, Hartings JA, Graf R, Strong AJ. Clinical relevance of cortical spreading depression in neurological disorders: migraine, malignant stroke, subarachnoid and intracranial hemorrhage, and traumatic brain injury. *J Cereb Blood Flow Metab* 2011; **31**: 17–35.
3 Somjen GG. Mechanisms of spreading depression and hypoxic spreading depression-like depolarization. *Physiol Rev* 2001; **81**: 1065–1096.
4 Czeh G, Aitken PG, Somjen GG. Membrane currents in CA1 pyramidal cells during spreading depression (SD) and SD-like hypoxic depolarization. *Brain Res* 1993; **632**: 195–208.
5 Dietz RM, Weiss JH, Shuttleworth CW. Zn2+ influx is critical for some forms of spreading depression in brain slices. *J Neurosci* 2008; **28**: 8014–8024.
6 Tottene A, Urbani A, Pietrobon D. Role of different voltage-gated Ca2+ channels in cortical spreading depression: specific requirement of P/Q-type Ca2+ channels. *Channels (Austin)* 2011; **5**: 110–114.
7 Menna G, Tong CK, Chesler M. Extracellular pH changes and accompanying cation shifts during ouabain-induced spreading depression. *J Neurophysiol* 2000; **83**: 1338–1345.
8 Zhou N, Gordon GR, Feighan D, MacVicar BA. Transient swelling, acidification, and mitochondrial depolarization occurs in neurons but not astrocytes during spreading depression. *Cereb Cortex* 2010; **20**: 2614–2624.
9 Corlew R, Brasier DJ, Feldman DE, Philpot BD. Presynaptic NMDA receptors: newly appreciated roles in cortical synaptic function and plasticity. *Neuroscientist* 2008; **14**: 609–625.
10 McGuinness L, Taylor C, Taylor RD, Yau C, Langenhan T, Hart ML *et al.* Presynaptic NMDARs in the hippocampus facilitate transmitter release at theta frequency. *Neuron* 2010; **68**: 1109–1127.
11 Larsen RS, Corlew RJ, Henson MA, Roberts AC, Mishina M, Watanabe M *et al.* NR3A-containing NMDARs promote neurotransmitter release and spike timing-dependent plasticity. *Nat Neurosci* 2011; **14**: 338–344.
12 Iijima T, Shimase C, Iwao Y, Sankawa H. Relationships between glutamate release, blood flow and spreading depression: real-time monitoring using an electro-enzymatic dialysis electrode. *Neurosci Res* 1998; **32**: 201–207.
13 Hoehn K, Watson TW, MacVicar BA. Multiple types of calcium channels in acutely isolated rat neostriatal neurons. *J Neurosci* 1993; **13**: 1244–1257.
14 Rossi DJ, Oshima T, Attwell D. Glutamate release in severe brain ischaemia is mainly by reversed uptake. *Nature* 2000; **403**: 316–321.
15 Warr O, Takahashi M, Attwell D. Modulation of extracellular glutamate concentration in rat brain slices by cystine-glutamate exchange. *J Physiol* 1999; **514**(Pt 3): 783–793.
16 Ye ZC, Wyeth MS, Baltan-Tekkok S, Ransom BR. Functional hemichannels in astrocytes: a novel mechanism of glutamate release. *J Neurosci* 2003; **23**: 3588–3596.
17 Zhou Q, Petersen CC, Nicoll RA. Effects of reduced vesicular filling on synaptic transmission in rat hippocampal neurones. *J Physiol* 2000; **525**(Pt 1): 195–206.
18 Cavelier P, Attwell D. Neurotransmitter depletion by bafilomycin is promoted by vesicle turnover. *Neurosci Lett* 2007; **412**: 95–100.
19 Ryan RM, Vandenberg RJ. Distinct conformational states mediate the transport and anion channel properties of the glutamate transporter EAAT-1. *J Biol Chem* 2002; **277**: 13494–13500.
20 Lo M, Wang YZ, Gout PW. The x(c)- cystine/glutamate antiporter: a potential target for therapy of cancer and other diseases. *J Cell Physiol* 2008; **215**: 593–602.
21 Iglesias R, Locovei S, Roque A, Alberto AP, Dahl G, Spray DC *et al.* P2 × 7 receptor-Pannexin1 complex: pharmacology and signaling. *Am J Physiol Cell Physiol* 2008; **295**: C752–C760.
22 Bruzzone R, Barbe MT, Jakob NJ, Monyer H. Pharmacological properties of homomeric and heteromeric pannexin hemichannels expressed in Xenopus oocytes. *J Neurochem* 2005; **92**: 1033–1043.
23 Sudhof TC. The presynaptic active zone. *Neuron* 2012; **75**: 11–25.
24 Nowak L, Bregestovski P, Ascher P, Herbet A, Prochiantz A. Magnesium gates glutamate-activated channels in mouse central neurones. *Nature* 1984; **307**: 462–465.
25 Lalo U, Pankratov Y, Kirchhoff F, North RA, Verkhratsky A. NMDA receptors mediate neuron-to-glia signaling in mouse cortical astrocytes. *J Neurosci* 2006; **26**: 2673–2683.
26 Palty R, Silverman WF, Hershfinkel M, Caporale T, Sensi SL, Parnis J *et al.* NCLX is an essential component of mitochondrial Na+/Ca2+ exchange. *Proc Natl Acad Sci USA* 2010; **107**: 436–441.
27 Perkins GA, Tjong J, Brown JM, Poquiz PH, Scott RT, Kolson DR *et al.* The micro-architecture of mitochondria at active zones: electron tomography reveals novel anchoring scaffolds and cristae structured for high-rate metabolism. *J Neurosci* 2010; **30**: 1015–1026.

28 Raiteri L, Zappettini S, Milanese M, Fedele E, Raiteri M, Bonanno G. Mechanisms of glutamate release elicited in rat cerebrocortical nerve endings by 'pathologically' elevated extraterminal K+ concentrations. *J Neurochem* 2007; **103**: 952–961.
29 Castaldo P, Cataldi M, Magi S, Lariccia V, Arcangeli S, Amoroso S. Role of the mitochondrial sodium/calcium exchanger in neuronal physiology and in the pathogenesis of neurological diseases. *Prog Neurobiol* 2009; **87**: 58–79.
30 Gerfen CL. *The Rat Nervous System*. 3 edn (Academic Press: Sydney; Orlando, 1985.
31 Castro JB, Urban NN. Subthreshold glutamate release from mitral cell dendrites. *J Neurosci* 2009; **29**: 7023–7030.
32 Schoppa NE, Urban NN. Dendritic processing within olfactory bulb circuits. *Trends Neurosci* 2003; **26**: 501–506.
33 Shepherd GM, Harris KM. Three-dimensional structure and composition of CA3-->CA1 axons in rat hippocampal slices: implications for presynaptic connectivity and compartmentalization. *J Neurosci* 1998; **18**: 8300–8310.
34 Fluegge D, Moeller LM, Cichy A, Gorin M, Weth A, Veitinger S *et al.* Mitochondrial Ca(2+) mobilization is a key element in olfactory signaling. *Nat Neurosci* 2012; **15**: 754–762.
35 Rizzuto R, De Stefani D, Raffaello A, Mammucari C. Mitochondria as sensors and regulators of calcium signalling. *Nat Rev Mol Cell Biol* 2012; **13**: 566–578.
36 Basarsky TA, Duffy SN, Andrew RD, MacVicar BA. Imaging spreading depression and associated intracellular calcium waves in brain slices. *J Neurosci* 1998; **18**: 7189–7199.
37 Santello M, Cali C, Bezzi P. Gliotransmission and the tripartite synapse. *Adv Exp Med Biol* 2012; **970**: 307–331.
38 Hubschmann OR, Kornhauser D. Cortical cellular response in acute subarachnoid hemorrhage. *J Neurosurg* 1980; **52**: 456–462.
39 Takahashi H, Manaka S, Sano K. Changes in extracellular potassium concentration in cortex and brain stem during the acute phase of experimental closed head injury. *J Neurosurg* 1981; **55**: 708–717.
40 Yang GY, Betz AL, Chenevert TL, Brunberg JA, Hoff JT. Experimental intracerebral hemorrhage: relationship between brain edema, blood flow, and blood-brain barrier permeability in rats. *J Neurosurg* 1994; **81**: 93–102.
41 Billups B, Attwell D. Modulation of non-vesicular glutamate release by pH. *Nature* 1996; **379**: 171–174.
42 Petzold GC, Windmuller O, Haack S, Major S, Buchheim K, Megow D *et al.* Increased extracellular K+ concentration reduces the efficacy of N-methyl-D-aspartate receptor antagonists to block spreading depression-like depolarizations and spreading ischemia. *Stroke* 2005; **36**: 1270–1277.
43 Ayata C, Shimizu-Sasamata M, Lo EH, Noebels JL, Moskowitz MA. Impaired neurotransmitter release and elevated threshold for cortical spreading depression in mice with mutations in the alpha1A subunit of P/Q type calcium channels. *Neuroscience* 2000; **95**: 639–645.
44 Tottene A, Conti R, Fabbro A, Vecchia D, Shapovalova M, Santello M *et al.* Enhanced excitatory transmission at cortical synapses as the basis for facilitated spreading depression in Ca(v)2.1 knockin migraine mice. *Neuron* 2009; **61**: 762–773.
45 Sakowitz OW, Kiening KL, Krajewski KL, Sarrafzadeh AS, Fabricius M, Strong AJ *et al.* Preliminary evidence that ketamine inhibits spreading depolarizations in acute human brain injury. *Stroke* 2009; **40**: e519–e522.
46 Hartings JA, Watanabe T, Bullock MR, Okonkwo DO, Fabricius M, Woitzik J *et al.* Spreading depolarizations have prolonged direct current shifts and are associated with poor outcome in brain trauma. *Brain* 2011; **134**: 1529–1540.

Supplementary Information accompanies the paper on the Journal of Cerebral Blood Flow & Metabolism website (http://www.nature.com/jcbfm)